Transactions Papers

Efficient Simulation of Digital Transmission over WSSUS Channels

Kun-Wah Yip and Tung-Sang Ng, *Senior Member, IEEE*

Abstract— **This paper proposes an efficient Monte Carlo method which reduces computation for digital communication simulations over a multipath Rayleigh fading, wide-sense-stationary uncorrelated-scattering (WSSUS) channel. An equivalent discrete-time channel representation, which can be realized by a FIR filter with time-variant tap gains, is employed. In the proposed method, the tap gains are generated from a linear transformation of a set of orthogonal zero-mean complex Gaussian random processes. By the central limit theorem, each random process is approximated by summing a finite number of randomly generated phasors (Monte Carlo approximation). When compared with the tap gain generation method described in earlier literature, which approximates the physical channel by the Monte Carlo approximation first and then generates the tap gain values, the proposed method demonstrates a considerable reduction in the required simulation time as well as improved accuracy under similar conditions.**

I. Introduction

Simulation of digital communications over multipath Rayleigh fading, wide-sense-stationary uncorrelated-scattering (WSSUS) channels is often computationally intensive as oversampling and extensive filtering are usually required. Recently, Hoeher [1] showed that considerable amount of computation could be reduced by using the equivalent discrete-time (EDT) channel representation, which can be realized by a FIR filter with time-variant tap gains [2, pp. 548–554], and by generating the tap gain values from the channel impulse response approximated by the Monte Carlo (MC) method [3]. This MC method approximates Rayleigh fading by summing a finite number of randomly generated phasors and invoking the central limit theorem.

Although not explicitly stated in [1] and [3], the MC approximation is applied to all Rayleigh-faded paths of the total multipath profile. The number of calculations is then proportional to the number of multipaths. As the number of tap gains is significantly lower than the total number of multipaths, potential reduction in the amount of computation is apparent if the MC approximation can be directly applied to the tap gains rather than the multipaths. Developing such an MC method is the objective of this paper.

The organization of this paper is as follows. Section II gives a brief review on the WSSUS channel model. A comprehensive discussion on this channel model is given by Bello [5]. Section III describes the continuous-time communication system model and its EDT channel model. The two models are equivalent in the sense that their input/output relationships are the same. Statistical properties of the tap gains of the EDT channel model, which are essential in the development of the proposed MC method, are also given. Section IV provides a short review on the MC method. Elaborate discussions on this method can be found in [1] and [3]. In Section V, we propose an efficient MC method which is directly applied to the tap gains. Comparison on computation times and accuracy between the proposed method and the method described in [1] is performed in Section VI. Finally, conclusions are given in Section VII.

II. WSSUS Channel Model

The fading dispersive channel can be characterized by the complex-valued, time-variant, low-pass equivalent channel impulse response $h(\tau;t)$. The value of $h(\tau;t)$ is the channel output at time t when an unit impulse is applied at $t-\tau$. For a WSSUS channel, the autocorrelation function of $h(\tau;t)$ is given by [5]

$$\tfrac{1}{2}\,E\{h(\tau_a;t)h^*(\tau_b;t+\Delta t)\} = \phi_h(\tau_a;\Delta t)\delta(\tau_b-\tau_a) \quad (1)$$

where $\phi_h(\tau;\Delta t)$ is the delay cross-power density. As a special case, $\phi_h(\tau;0) \triangleq Q(\tau)$ is known as the delay power spectrum and without loss of generality, it is assumed that $Q(\tau)=0$ for $\tau<0$. The Fourier transform of $\phi_h(\tau;\Delta t)$ on the variable Δt, given by

$$S_h(\tau;\lambda) = \int_{-\infty}^{\infty} \phi_h(\tau;\Delta t)e^{-j2\pi\lambda(\Delta t)}\,d\Delta t \quad (2)$$

is known as the scattering function of the channel. Taking Fourier transform on τ again yields

$$S_H(\Delta f;\lambda) = \int_{-\infty}^{\infty} S_h(\tau;\lambda)e^{-j2\pi(\Delta f)\tau}\,d\tau. \quad (3)$$

Paper approved by K. Townsend, the Editor for Computer-Aided Design of Communication Systems of the IEEE Communications Society. Manuscript received May 23, 1994; revised February 2, 1995. This work was supported by the CRCG of the University of Hong Kong, and by the HKRGC.

The authors are with the Department of Electrical and Electronic Engineering, The University of Hong Kong, Hong Kong.

IEEE Log Number 9414701.

0090–6778/95$04.00

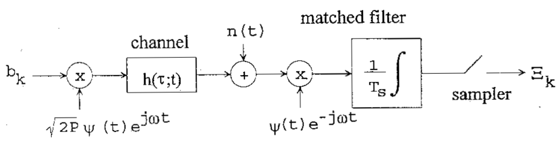

Fig. 1. The continuous-time communication system model.

The function $S_H(0;\lambda) \triangleq S(\lambda)$ is known as the Doppler power spectrum.

Most often the multipath dispersion, which depends on the distribution of scatterers within the communication medium, and the Doppler variation, which is usually dependent on the relative motion between the transmitter and receiver, are independent events. We therefore assume that $S_h(\tau;\lambda)$ can be factored into $S_h(\tau;\lambda) = A(\tau)B(\lambda)$. Since

$$\begin{aligned}\phi_h(\tau;\Delta t) &= \int_{-\infty}^{\infty} S_h(\tau;\lambda)e^{j2\pi\lambda(\Delta t)}\,d\lambda\\ &= A(\tau)\int_{-\infty}^{\infty} B(\lambda)e^{j2\pi\lambda(\Delta t)}\,d\lambda,\\ Q(\tau) &= \phi_h(\tau;0) = A(\tau)\int_{-\infty}^{\infty} B(\lambda)\,d\lambda \quad \text{and}\\ S(\lambda) &= S_H(0;\lambda) = B(\lambda)\int_{-\infty}^{\infty} A(\tau)\,d\tau\end{aligned}$$

it follows that

$$\phi_h(\tau;\Delta t) = Q(\tau)\frac{\int_{-\infty}^{\infty} S(\lambda)e^{j2\pi\lambda(\Delta t)}\,d\lambda}{\int_{-\infty}^{\infty} S(\lambda)\,d\lambda} \tag{4}$$

assuming $\int_{-\infty}^{\infty} S(\lambda)\,d\lambda \neq 0$. This result will be used later in the development of the EDT channel model.

III. Continuous-Time Communication System and its EDT Channel Model

The continuous-time communication system model is shown in Fig. 1. It is the same as the model described in [4]. The complex-valued transmitted signal,[1] $r(t)$, is given by $r(t) = u(t)e^{j\omega t}$, where ω is the carrier frequency, and

$$u(t) = \sqrt{2P}\sum_{m=-\infty}^{\infty} b_m\psi(t - mT_s). \tag{5}$$

In the expression, P is the signal power, b_m is the mth transmitted symbol where $E\{b_m b_m^*\} = 1$, T_s is the symbol time, $\psi(t)$ is the real-valued symbol waveform, time-limited within $[0, T_s)$ and satisfied $\int_0^{T_s}\psi^2(t)\,dt = T_s$. The signal $r(t)$ is transmitted through a multipath Rayleigh fading WSSUS channel $h(\tau;t)$. Therefore, $h(\tau;t)$ follows a zero-mean complex Gaussian random process in the t variable. At the receiver, the received signal, $s(t)$, is given by

$$s(t) = n(t) + e^{j\omega t}\int_{-\infty}^{\infty} u(t-\tau)h(\tau;t)\,d\tau \tag{6}$$

[1] In this paper, complex signal representations are used. The physical signal can be obtained by taking the real part of the corresponding complex signal.

where $n(t)$ is the complex AWGN with one-sided noise power spectral density η, i.e., $\frac{1}{2}E\{n(t)n^*(t+\tau)\} = \eta\cdot\delta(\tau)$. A matched filter matched to the transmitted symbol waveform is used to process $s(t)$ and a sampler is followed. The complex-valued matched filter output at the kth sampling instant, Ξ_k, is given by

$$\Xi_k = (T_s)^{-1}\int_{kT_s}^{(k+1)T_s} s(t')\psi(t' - kT_s)e^{-j\omega t'}\,dt'. \tag{7}$$

Notice that the matched filter output is sampled at the instant $(k+1)T_s$.

The EDT channel model (Fig. 2) is equivalent to the continuous-time communication system model in the input/output relationship. In the EDT channel model, Ξ_k is related to b_k by

$$\Xi_k = N_k + \sqrt{2P}\sum_{m=0}^{M-1} b_{k-m}g_m(t) \tag{8}$$

where (i) N_k is the complex Gaussian distributed noise, (ii) $g_m(t)$ is the complex-valued time-variant tap gain and it is assumed that there are only M tap gains. The dependence of $g_m(t)$ on t indicates the time-varying behavior of the tap gain; but in simulations, only tap gain values at the kth sampling instant, i.e., $g_m((k+1)T_s)$, are necessary in evaluating Ξ_k. In Appendix I, it is shown that (i) $\{N_k\}$ is a statistically independent, zero-mean complex Gaussian noise sequence with $E\{N_kN_k^*\} = 2\eta/T_s$; (ii)

$$g_m(t) = \int_{-\infty}^{\infty} h(\tau;t)\cdot W(mT_s - \tau)\,d\tau \tag{9}$$

where

$$W(\tau) = (T_s)^{-1}\int_0^{T_s}\psi(t')\psi(t'+\tau)\,dt'$$

so that $g_0(t), g_1(t), \cdots, g_{M-1}(t)$ follow a multivariate, zero-mean complex Gaussian random process with

$$\begin{aligned}&E\{g_m(t)g_n^*(t+\Delta t)\}\\ &\quad= \int_{-\infty}^{\infty} 2\phi_h(\tau;\Delta t)W(mT_s-\tau)W(nT_s-\tau)\,d\tau,\\ &\qquad m,n \in \{0,1,\cdots,M-1\}.\end{aligned} \tag{10}$$

In deriving (9) and (10), it is assumed that channel fading is slowly varying such that for a particular $\tau, h(\tau;t)$ is approximately constant during the interval $kT_s \le t \le (k+1)T_s$. This assumption implies that the coherence time of the channel is much greater than T_s seconds, and is usually satisfied. Substituting (4) into (10) gives

$$\begin{aligned}&E\{g_m(t)g_n^*(t+\Delta t)\}\\ &\quad= E\{g_m(t)g_n^*(t)\}\frac{\int_{-\infty}^{\infty} S(\lambda)e^{j2\pi\lambda(\Delta t)}\,d\lambda}{\int_{-\infty}^{\infty} S(\lambda)\,d\lambda}\end{aligned} \tag{11}$$

where

$$E\{g_m(t)g_n^*(t)\} = \int_{0^-}^{\infty} 2Q(\tau)W(mT_s-\tau)W(nT_s-\tau)\,d\tau. \tag{12}$$

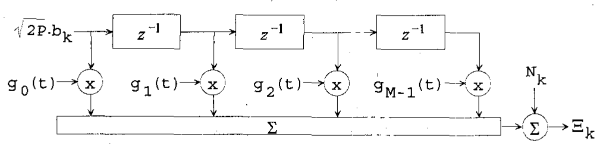

Fig. 2. The equivalent discrete-time channel model.

Equation (12) was already derived in [4], where emphasis was predominantly given to the effect of channel dispersion on $g_m(t)$ rather than the temporal fading behavior of the tap gains. Several properties can be deduced from (12): $E\{g_m(t)g_n^*(t)\}$ is real-valued as $Q(\tau) \in \mathbb{R}$ and $W(\tau) \in \mathbb{R}$; $E\{g_m(t)g_n^*(t)\} = E\{g_n(t)g_m^*(t)\}$; the tap gains are statistically correlated as $E\{g_m(t)g_{m+1}^*(t)\} \neq 0$ in general, which was also reported in [4].

IV. Review of the MC Method

For the MC method, $h(\tau;t)$ is approximated by [1], [3]

$$h_N(\tau;t) = \frac{1}{\sqrt{N}} \sum_{n=0}^{N-1} e^{j(\theta_n - 2\pi\lambda_m t)} \delta(\tau - \tau_n) \tag{13}$$

where (i) N is the number of random phasors, (ii) $\theta_n \forall n$ are independently identically distributed (i.i.d.) random variables uniformly distributed over $[0, 2\pi)$, (iii) $\tau_n \forall n$ are i.i.d. random variables with pdf $p(\tau) \triangleq p(\tau_n)$ given by

$$p(\tau) = Q(\tau) \Big/ \int_{-\infty}^{\infty} Q(\tau')\, d\tau' \tag{14}$$

(iv) $\lambda_n \forall n$ are i.i.d. random variables with pdf $p(\lambda) \triangleq p(\lambda_n)$ given by

$$p(\lambda) = S(\lambda) \Big/ \int_{-\infty}^{\infty} S(\lambda')\, d\lambda'. \tag{15}$$

As N approaches infinity, $h_N(\tau;t)$ becomes $h(\tau;t)$ and by the central limit theorem, $|h_N(\tau',t)|$ follows Rayleigh fading for every τ'. After $h_N(\tau;t)$ is generated, $g_m(t)$ can be computed by (9) with $h(\tau;t)$ approximated by $h_N(\tau;t)$, and Ξ_k can be calculated by (8).

In general, the amount of computation is proportional to the number of Rayleigh-faded paths considered sufficient in modeling the channel dispersion. This is explained as follows. We first divide the axis τ of $h(\tau;t)$ into segments at points $\{\tau_i''\}$ such that $\int_{\tau_i''}^{\tau_{i+1}''} Q(\tau)\, d\tau \forall i$ are equal. In addition, $\Delta\tau_i'' \triangleq \tau_{i+1}'' - \tau_i''$ can be made arbitrarily small such that a single Rayleigh-faded path can be considered sufficient in representing the contribution of $h(\tau;t)$ within $\Delta\tau_i''$. In the MC method, $h(\tau;t)$ is approximated by $h_N(\tau;t)$. For each Rayleigh-faded path, Rayleigh fading is approximated by summing all random phasors within $\Delta\tau_i''$. It can be shown that in the generation of $h_N(\tau;t)$, the number of random phasors in the segment $\Delta\tau_i''$ is on the average equal to $N \int_{\tau_i''}^{\tau_{i+1}''} p(\tau)\, d\tau$. The condition of equal $\int_{\tau_i''}^{\tau_{i+1}''} Q(\tau)\, d\tau \forall i$ implies that $\int_{\tau_i''}^{\tau_{i+1}''} p(\tau)\, d\tau$ are also equal $\forall i$; therefore, we let $P_{\text{path}} = \int_{\tau_i''}^{\tau_{i+1}''} p(\tau)\, d\tau$. Since $\Sigma_i \int_{\tau_i''}^{\tau_{i+1}''} p(\tau)\, d\tau = 1$, it follows that $P_{\text{path}} = 1/N_{\text{SP}}$, where N_{SP} is the number of segments in dividing the axis τ. Notice that as there is one Rayleigh-faded path in each segment, N_{SP} is also the number of Rayleigh-faded paths over the whole channel dispersion. Next, the condition of equal $\int_{\tau_i''}^{\tau_{i+1}''} p(\tau)\, d\tau \forall i$ implies that the number of random phasors in each segment is on the average the same. Let N_{RAY} be the average number of random phasors in each segment. This number N_{RAY} can be taken as a constant and its value is primarily determined by how close Rayleigh fading is to be approximated for each Rayleigh-faded path. Since $N_{\text{RAY}} = N \int_{\tau_i''}^{\tau_{i+1}''} p(\tau)\, d\tau = P_{\text{path}} N$, it immediately gives $N = N_{\text{RAY}} N_{\text{SP}}$. Therefore, the amount of computation is proportional to the number of Rayleigh-faded paths.

V. An Efficient MC Method

The proposed MC method aims at generating the tap gain values directly without first generating $h_N(\tau;t)$. Since $g_m(t)$ is a zero-mean complex Gaussian random process, an appropriate function capable of generating this random process is required. The generating function, $f_N(t)$, is defined as

$$f_N(t) = \frac{1}{\sqrt{N}} \sum_{n=0}^{N-1} e^{j(\theta_n - 2\pi\lambda_n t)} \tag{16}$$

where θ_n and λ_n follow the same definitions in defining $h_N(\tau;t)$ in (13). By the central limit theorem, $f(t) \triangleq \lim_{N\to\infty} f_N(t)$ is a zero-mean complex Gaussian random process; but for most practical purposes, a small value of N ($N = N_{\text{RAY}}$) is sufficient in obtaining a good approximation of $f(t)$. Since there are M tap gains, the amount of computation is proportional to MN_{RAY}, or alternatively, proportional to the number of tap gains. As the number of tap gains is in general substantially less than the number of Rayleigh-faded paths, it is apparent that considerable amount of computation effort can be reduced when compared with the MC method described in [1] and [3].

A. Generation of $g_m(t)$

For any integer m, let $f_N(t;m)$ take the value of $f_N(t)$ according to (16) and $f(t;m) \triangleq \lim_{N\to\infty} f_N(t;m)$. In addition, $f_N(t;m_1)$ and $f_N(t;m_2), m_1 \neq m_2$, are generated from independent sets of $\{\theta_n, \lambda_n\}$ so that $E\{f_N(t;m_1)f_N^*(t+\Delta t;m_2)\} = 0$. For the sake of convenience, $E\{g_m(t)g_n^*(t)\}$ is denoted by $a_{m,n}$, and $\boldsymbol{A}$ is an $M \times M$ matrix[2] with elements $a_{m,n}$ for $m,n \in \{0,1,\cdots,M-1\}$. Note that $\boldsymbol{A}$ is the covariance matrix of $\{g_m(t)\}$ for $m \in \{0,1,\cdots,M-\}$. Then the tap gains $g_m(t)\forall m$ can be generated by

$$\boldsymbol{G}(t) = \boldsymbol{C}\boldsymbol{F}(t) \tag{17}$$

where (i) $\boldsymbol{G}(t) = [g_0(t), g_1(t), \cdots, g_{M-1}(t)]^T$, (ii) $\boldsymbol{F}_N(t) = [f_N(t;0), f_N(t;1), \cdots, f_N(t;M-1)]^T$ and $\boldsymbol{F}(t) = \lim_{N\to\infty} \boldsymbol{F}_N(t)$, (iii) $\boldsymbol{C}$ is an $M \times M$ matrix with (m,n)th element $c_{m,n} \in \mathbb{R}$, and satisfies the relationship

$$\boldsymbol{A} = \boldsymbol{C}\boldsymbol{C}^T. \tag{18}$$

[2]Throughout this paper, the upper left element of a matrix is assigned an index number (0, 0) rather than the common convention (1, 1).

Proof: It is apparent that the R.H.S. of (17) generates a multivariate, zero-mean complex Gaussian random process. Then it is sufficient to find the matrix $\boldsymbol{C}$ such that (11) is satisfied $\forall m, n \in \{0, 1, \cdots, M-1\}$. From (17), $g_m(t) = \Sigma_{u=0}^{M-1} c_{m,u} f(t;u)$, and it follows that

$$E\{g_m(t)g_n^*(t+\Delta t)\} = \sum_{u=0}^{M-1}\sum_{v=0}^{M-1} c_{m,u}c_{n,v}^* \cdot E\{f(t;u)f^*(t+\Delta t;v)\}. \quad (19)$$

It is shown in the Appendix II that

$$E\{f_N(t)f_N^*(t+\Delta t)\} = \frac{\int_{-\infty}^{\infty} S(\lambda)e^{j2\pi\lambda(\Delta t)}\,d\lambda}{\int_{-\infty}^{\infty} S(\lambda)\,d\lambda}. \quad (20)$$

After equating (11) and (19), it follows that

$$E\{g_m(t)g_n^*(t)\} = \sum_{u=0}^{M-1} c_{m,u}c_{n,u}^*, \quad \forall m, n \in \{0, 1, \cdots, M-1\}. \quad (21)$$

Hence, $\boldsymbol{C}$ satisfies the relationship $\boldsymbol{A} = \boldsymbol{C}(\boldsymbol{C}^*)^T$. Since the covariance matrix $\boldsymbol{A}$ is real symmetric ($a_{m,n} \in \mathbb{R}$ and $a_{m,n} = a_{n,m}$) and positive semidefinite [6, ch. 22.3], $\boldsymbol{A}$ can be factored into $\boldsymbol{A} = \boldsymbol{X}\boldsymbol{X}^T$ where $\boldsymbol{X}$ is a real $M \times M$ matrix. Consequently, the matrix $\boldsymbol{C}$ can be found by any factor of $\boldsymbol{A}$ satisfying $\boldsymbol{A} = \boldsymbol{C}\boldsymbol{C}^T$ with $c_{m,n} \in \mathbb{R}\,\forall m, n$. □

Notice that all the elements $\boldsymbol{F}(t)$ of follow *orthogonal*, zero-mean complex Gaussian random processes, and $\boldsymbol{G}(t)$ is generated by a linear transformation of $\boldsymbol{F}(t)$.

B. Implementation Aspects

In the implementation of the proposed MC method, the first step is to determine an appropriate value of M so that Ξ_k can be accurately computed. To achieve the desired accuracy, it is necessary to include sufficient number of terms in the computation of Ξ_k using (8). As a general rule, the value of M can be determined by including all terms whose $E\{g_m(t)g_m^*(t)\}$ values are considered large. Although including more terms generally improves accuracy in the computation of Ξ_k, the improvement diminishes in general as M increases. In addition, the computation time is longer for a higher value of M as the amount of computation is proportional to M. It is therefore important to select an appropriate value of M in order to avoid loss of accuracy and the need of excessive computation time.

After M is determined, the covariance matrix $\boldsymbol{A}$ can be constructed with elements computed by (12). The integration involved in (12) can be evaluated analytically or computed numerically. There are available tools and programming aids, such as MATHEMATICA and IMSL library routines, which allow fast evaluation of the integral symbolically or numerically. Therefore $\boldsymbol{A}$ can be readily generated. Then $\boldsymbol{C}$ can be obtained by factorizing $\boldsymbol{A}$ according to (18). In general, factorization of $\boldsymbol{A}$ is not unique and different factorization methods yield different $\boldsymbol{C}$'s which satisfy (18). For simulation purposes, $\boldsymbol{C}$ is preferred to be a lower triangular matrix as some of the steps in multiplication and addition can be eliminated. This minimizes the amount of computation. The factorization of $\boldsymbol{A}$ can be efficiently accomplished by Cholesky factorization. After $\boldsymbol{C}$ is obtained, $\boldsymbol{G}(t)$ can be generated from $\boldsymbol{F}(t)$ by applying (17). Although $\boldsymbol{F}(t)$ can only be obtained by summing an infinite number of randomly generated phasors, it can be closely approximated by $\boldsymbol{F}_N(t)$ with a finite and usually small value of N. (It is well known that $N \geq 6$ is generally sufficient [7, pp. 68–69].) After the random seeds θ_n and λ_n for $0 \leq n \leq N-1$ are generated according to their respective pdf's, $\boldsymbol{F}_N(t)$ can be readily computed. It can be shown that $f_N(t;m)$ is non-periodic if there exists λ_{n1} and λ_{n2} such that $\lambda_{n1}/\lambda_{n2}$ is an irrational number (Appendix III). As λ_n's are randomly generated, this condition is easily satisfied.[3] Therefore, it is sufficient to generate the random seeds once only to produce a non-repeating function $\boldsymbol{F}_N(t)$. However, regeneration of random seeds after a certain number of simulation runs is recommended for small N in order to improve the statistics of $\boldsymbol{F}_N(t)$. Notice that the generation of $\boldsymbol{A}, \boldsymbol{C}$ and possibly the random seeds is done once only, and takes up a small fraction of the total simulation time. On the other hand, the generation of $\boldsymbol{F}_N(t)$ and $\boldsymbol{G}(t)$ often dominates the simulation time as the number of runs in simulation is usually enormous. This is the advantage of the proposed MC method as it provides a computationally efficient method in the generation of $\boldsymbol{F}_N(t)$ and $\boldsymbol{G}(t)$. Finally, Ξ_k can be computed by (8). Also notice that it is only necessary to generate values of $\boldsymbol{G}(iT_s), i$ an integer, in the computation of $\{\Xi_k\}$ as $\Xi_k \forall k$ are discrete-time outputs obtained at a rate of $1/T_s$ per second.

VI. Comparison Results

In order to compare computational times and accuracy between the MC method of [1] and the proposed one, simulation runs were performed in generating the tap gain values for a typical WSSUS channel with exponential multipath intensity profile

$$Q(\tau) = (2\tau_{\rm rms})^{-1}\exp(-\tau/\tau_{\rm rms}), \qquad \tau \geq 0$$

where $\tau_{\rm rms}$ is the rms delay spread of the channel. This channel dispersion model is commonly accepted in modeling certain types of mobile radio channels [8]. For simplicity, it was assumed that $\tau_{\rm rms} = T_s$ so that most of the channel dispersion was concentrated within $\tau \leq 4T_s$.

In the MC method of [1], it was required to specify the number of Rayleigh-faded paths $N_{\rm SP}$ which could be considered sufficient in representing the channel dispersion (Section IV). Three cases of $N_{\rm SP}$ (10, 20, 40) were considered. Notice that the channel might not be adequately represented by 10 Rayleigh-faded paths over a dispersion of $4T_s$, but the number of computation was minimum among the three cases. Therefore, extra effort is required to identify a suitable value of $N_{\rm SP}$ before applying the MC method of [1]. This step is,

[3] In a computer, λ_n's can only be stored with a finite number of digits so that they are not irrational numbers. As a result, $f_N(t;m)$ is periodic; but its period is very long and practically $f_N(t;m)$ can be treated as non-periodic.

TABLE I
SIMULATION TIMES TAKEN FOR 10^5 SIMULATION RUNS USING (a) THE MC METHOD OF [1] WITH THE NUMBER OF RAYLEIGH-FADED PATHS $N_{SP} = 10, 20, 40$ AND (b) THE PROPOSED MC METHOD. THE VALUES IN THE BRACKETS ARE NORMALIZED VALUES FOR COMPARISON PURPOSE

		Simulation time	
(a)	$N_{SP} = 10$	730.2 s	(1.61)
	$N_{SP} = 20$	1253.4 s	(2.76)
	$N_{SP} = 40$	2560.0 s	(5.63)
(b)		454.5 s	(1.00)

however, not necessary in the proposed MC method and this is certainly an advantage.

The remaining simulation conditions are given as follows. The Doppler variation of the channel was assumed to follow the Jakes spectrum [7] with maximum Doppler frequency $1/(100T_s)$ Hz; hence $S(\lambda) = [\pi\lambda_{\max}\sqrt{1-(\lambda/\lambda_{\max})^2}]^{-1}$ where $\lambda_{\max}^{-1} = 100T_s$. In approximating Rayleigh fading, the number of random phasors for summation was assumed to be $N_{RAY} = 10$. For the MC method of [1], $N = 100$, 200, 400 were used in the construction of $h_N(\tau;t)$ as $N = N_{SP}N_{RAY}$. For the proposed method, $N = 10$ was employed in the generation of $f_N(t;m)$ because $N = N_{RAY}$. Five tap gains were generated in a run and a total of 10^5 runs were simulated, yielding $g_m(kT_s)$, where $0 \le m \le 4$ and $1 \le k \le 10^5$, for both MC methods. Rectangular symbol waveform was assumed. A SUN SPARC 2 workstation was used in the simulation of both MC methods and the two simulation programs were written in MATLAB.

The simulation times required for both MC methods are listed in Table I. The required simulation times for the MC method of [1] are 1.61–5.63 times that of the proposed MC method. The proposed method is more efficient, and the advantage would be even more obvious when it is necessary to generate $h_N(\tau;t)$ with a higher value of N_{SP} in the MC method of [1]. The comparison results demonstrate the efficiency of the proposed method.

Next, we compare the accuracy of the proposed method with the MC method of [1]. If the samples are accurately generated, then for each m, the cumulative relative frequency function (c.r.f.f.) of samples $|g_m(kT_s)|, 1 \le k \le 10^5$, should follow the cumulative density function (c.d.f.) of Rayleigh distribution with variance $E\{g_m(t)g_m^*(t)\}$. Fig. 3(a) and (b) plot the c.r.f.f.'s, $m \in \{0, 1, \cdots, 4\}$, of samples generated by the MC method of [1] with $N_{SP} = 10$ and the proposed MC method, respectively. The choice of $N_{SP} = 10$ is to facilitate comparison on the basis of roughly the same computation times. Also plotted in the figures are the c.d.f.'s of Rayleigh distributions with variance $E\{g_m(t)g_m^*(t)\}$. For the MC method of [1], it is apparent that generated samples fit well to Rayleigh distributions in cases $m \in \{0, 1\}$ but deviate significantly from Rayleigh statistics for $m \in \{2, 3\}$ and especially for $m = 4$. On the other hand, c.r.f.f.'s in all cases of m follow closely to their respective c.d.f.'s for the proposed MC method, indicating that Rayleigh statistics are closely approximated for all tap gains. The comparison indicates that on the basis of roughly the same computation times, accuracy of the proposed method is better than that of the MC method proposed in [1].

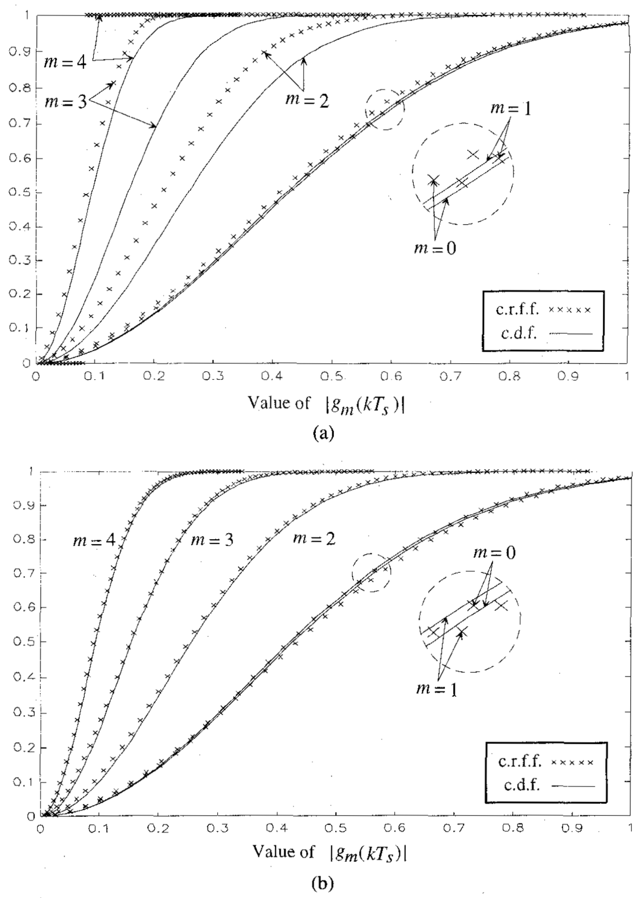

Fig. 3. Cumulative relative frequency functions (c.r.f.f.) of samples $|g_m(kT_s)|, 1 \le k \le 10^5$, generated by (a) the MC method of [1] with $N_{SP} = 10$ and (b) the proposed MC method. Also plotted are cumulative density functions (c.d.f.) of Rayleigh distributions with variance $E\{g_m(t)g_m^*(t)\}$.

As a further remark, it is found that regeneration of random seeds $(\theta_n, \lambda_n, \tau_n)$ can improve accuracy of both MC methods, but the samples generated by the proposed method converge faster to Rayleigh distributions than the MC method of [1]. Apart from comparison on amplitude distributions of generated samples, we have also compared (i) phase distributions, (ii) sample correlations of $g_m(kT_s)$ and $g_m((k + \Delta k)T_s)$ for different Δk, and (iii) sample correlations of $g_m(kT_s)$ and $g_n(kT_s)$ for $m \ne n$. Similar conclusions have been reached.

VII. CONCLUSIONS

An efficient MC method, which requires less computation than the MC method described in [1], has been proposed. The proposed method computes the time-variant tap gains of the EDT channel model by a linear transformation of a set of orthogonal zero-mean complex Gaussian random processes, and each process is approximated by summing a finite number of randomly generated phasors. In a comparison, it has been shown that the proposed method requires less computation time and provides better accuracy than the MC method of [1] in the generation of tap gain values for a typical channel.

APPENDIX I
DEVELOPMENT OF THE EDT CHANNEL MODEL

Expressions of N_k and $g_m(t)$ are derived as follows. First notice that in the evaluation of Ξ_k using (8), the value of $g_m(t)$ is indeed $g_m((k+1)T_s)$ since sampling is taken at time $t=(k+1)T_s$. Expressions of N_k and $g_m((k+1)T_s)$ can be derived by rewriting (5) as $u(t)=\sqrt{2P}\,\Sigma_{m=-\infty}^{\infty} b_{k-m}\psi(t-(k-m)T_s)$ and evaluating the expression of Ξ_k using (6) and (7), followed by comparison with (8). Then the expression of $g_m(t)$ can be obtained by substituting $(k+1)T_s=t$ into the expression of $g_m((k+1)T_s)$. It follows that

$$N_k=(T_s)^{-1}\int_{kT_s}^{(k+1)T_s} n(t')\psi(t'-kT_s)e^{-j\omega t'}\,dt' \quad \text{(A1)}$$

and

$$\begin{aligned} g_m((k+1)T_s) &= (T_s)^{-1}\int_{kT_s}^{(k+1)T_s}\int_{-\infty}^{\infty}\psi(t'-\tau-(k-m)T_s)\\ &\quad\cdot\psi(t'-kT_s)h(\tau;t')\,d\tau\,dt'. \end{aligned} \quad \text{(A2)}$$

Therefore, $\{N_k\}$ is a zero-mean complex Gaussian noise sequence. Since $\frac{1}{2}E\{n(t)n^*(t+\tau)\}=\eta\cdot\delta(\tau)$, it is easy to show that $E\{N_kN_k^*\}=2\eta/T_s$ and $E\{N_kN_{k'}^*\}=0\,\forall k\neq k'$. The latter result implies that $N_k\,\forall k$ are statistically independent. Next, (A2) can be simplified by assuming that $h(\tau;t')$ is approximately constant during $kT_s\leq t'\leq(k+1)T_s$ for a particular τ. Substituting $h(\tau;t')\approx h(\tau;(k+1)T_s)$ into (A2), we obtain $g_m((k+1)T_s)=\int_{-\infty}^{\infty}h(\tau;(k+1)T_s)\cdot W(mT_s-\tau)\,d\tau$, where $W(\tau)=(T_s)^{-1}\int_0^{T_s}\psi(t')\psi(t'+\tau)\,dt'$. Substituting $(k+1)T_s=t$ into $g_m((k+1)T_s)$ gives

$$g_m(t)=\int_{-\infty}^{\infty}h(\tau;t)\cdot W(mT_s-\tau)\,d\tau. \quad \text{(A3)}$$

Therefore, $g_0(t),g_1(t),\cdots,g_{M-1}(t)$ follow a multivariate, zero-mean complex Gaussian random process and can be characterized with a knowledge of $E\{g_m(t)g_n^*(t+\Delta t)\},m,n\in\{0,1,\cdots,M-1\}$. Substituting (A3) into $E\{g_m(t)g_n^*(t+\Delta t)\}$ followed by an application of (1), (10) is readily obtained.

APPENDIX II
PROOF OF (20)

By algebraic expansion, it is easy to show that

$$\begin{aligned} f_N(t)f_N^*(t+\Delta t) &= \frac{1}{N}\sum_{n=0}^{N-1}e^{j(2\pi\lambda_n\Delta t)}+\frac{1}{N}\sum_{m\neq n}\\ &\quad\cdot e^{j[\theta_m-\theta_n-2\pi(\lambda_m-\lambda_n)t+2\pi\lambda_n\Delta t]}. \end{aligned} \quad \text{(A4)}$$

Let $U=\theta_m-\theta_n$ and $V=-2\pi(\lambda_m-\lambda_n)t+2\pi\lambda_n\Delta t$. Since

$$\begin{aligned}\exp j(U+V) &= \cos U\cos V-\sin U\sin V\\ &\quad+j(\sin U\cos V+\cos U\sin V)\end{aligned}$$

and $E\{\sin U\}=E\{\cos U\}=0$, it follows that the expectation value of the latter part of (A4) is zero. Therefore,

$$\begin{aligned} E\{f_N(t)f_N^*(t+\Delta t)\} &= E\left\{\frac{1}{N}\sum_{n=0}^{N-1}e^{j(2\pi\lambda_n\Delta t)}\right\}\\ &= \int_{-\infty}^{\infty}p(\lambda)e^{j(2\pi\lambda\Delta t)}\,d\lambda. \end{aligned} \quad \text{(A5)}$$

The last expression is obtained since $\lambda_0,\lambda_1,\cdots,\lambda_{N-1}$ are i.i.d. random variables with pdf $p(\lambda)=p(\lambda_n)\forall n$. Applying $p(\lambda)=S(\lambda)/\int_{-\infty}^{\infty}S(\lambda')\,d\lambda'$ to (A5), (20) is readily established.

APPENDIX III
NON-PERIODIC CHARACTERISTIC OF $f_N(t;m)$

If there exists a pair of random seeds, λ_{n1} and λ_{n2}, such that $\lambda_{n1}/\lambda_{n2}$ is an irrational number, then $f_N(t;m)$ is non-periodic. The proof is given as follows. Suppose that $f_N(t;m)$ is periodic with period denoted by T_p, i.e., $f_N(t+T_p;m)=f_N(t;m)$, and neglect the trivial case of $T_p=0$. Equating $f_N(t+T_p;m)=f_N(t;m)$ and noting that $f_N(t;m)$ is given by (16), the following result is obtained:

$$\sum_{n=0}^{N-1}e^{j(\theta_n-2\pi\lambda_nt)}\{1-e^{-j2\pi\lambda_nT_p}\}=0.$$

This is true only if $1-\exp(-j2\pi\lambda_nT_p)=0\,\forall n\in\{0,1,\cdots,N-1\}$. Consequently, there exists $\ell_0,\ell_1,\cdots,\ell_{N-1}\in\mathbb{Z}$ such that $2\pi\lambda_nT_p=2\pi\ell_n\,\forall n$. It follows that $\lambda_{n1}T_p=\ell_{n1}$ and $\lambda_{n2}T_p=\ell_{n2}$. Since $\lambda_{n1}/\lambda_{n2}$ is an irrational number, λ_{n1} and λ_{n2} are both non-zero. As $T_p\neq 0$, it follows that ℓ_{n1} and ℓ_{n2} are also non-zero. Division of the two expressions gives $\lambda_{n1}/\lambda_{n2}=\ell_{n1}/\ell_{n2}$, which is a rational number. This results in a contradiction. Consequently, $f_N(t;m)$ is non-periodic.

ACKNOWLEDGMENT

The authors are indebted to Mr. C. Y. Vong for his helpful comments on the earlier version of the manuscript; they also thank the anonymous reviewers for various useful comments and suggestions.

REFERENCES

[1] P. Hoeher, "A statistical discrete-time model for the WSSUS multipath channel," *IEEE Trans. Veh. Technol.*, vol. 41, pp. 461–468, Nov. 1992.

[2] J. G. Proakis, *Digital Communications*, 2nd ed. New York: McGraw-Hill, 1989.

[3] H. Schulze, "Stochastic models and digital simulation of mobile channels" (in German), in *Proc. Kleinheubacher Berichte by the German PTT*, 1989, pp. 473–483.

[4] K. W. Yip and T. S. Ng, "An analytic discrete-time model for a fading dispersive WSSUS channel," in *44th IEEE Veh. Technol. Soc. Conf.*, 1994.

[5] P. A. Bello, "Characterization of randomly time-variant linear channels," *IEEE Trans. Commun. Syst.*, vol. CS-11, pp. 360–393, Dec. 1963.

[6] H. Cramér, *Mathematical Methods of Statistics*. Princeton, NJ: Princeton University Press, 1945.

[7] W. C. Jakes, Ed., *Microwave Mobile Communications*. New York: Wiley, 1974.

[8] W. C. Y. Lee, *Mobile Communications Design Fundamentals*. New York: Howard W. Sams, 1986.

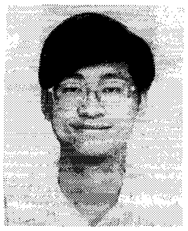

Kun-Wah Yip was born in Hong Kong on May 28, 1968. He received the B.Eng. (Hons) degree in electrical and electronic engineering from The University of Bradford, UK, in 1991.

He is with The University of Hong Kong, working towards his Ph.D. degree in the area of direct sequence spread spectrum multiple access communications over fading dispersive channels. His current interests include spread-spectrum techniques and mobile communications.

Tung-Sang Ng (S'74–M'78–SM'90) received the B.Sc. (Eng.) degree from The University of Hong Kong, in 1972, and the M.Eng.Sc. and Ph.D. degrees from The University of Newcastle, Australia, all in electrical engineering, in 1974 and 1977, respectively.

He was employed as an electrical engineer by BHP Newcastle Iron and Steel Works, Australia, from 1972 to 1974. From 1977 to 1990, he was with the Department of Electrical and Computer Engineering, The University of Wollongong, Australia, as a member of the academic staff. He is currently a Professor of Electronic Engineering at the University of Hong Kong. His current research interests include spread spectrum techniques, digital signal processing, mobile communication systems and engineering applications of artificial intelligence. He is a regional editor for an INTERNATIONAL JOURNAL—ENGINEERING APPLICATIONS OF ARTIFICIAL INTELLIGENCE (Pergamon Press).

Dr. Ng is a senior member of IEEE, and a fellow of both IEE and IEAust.